

# PATH UNCERTAINTY ROBUST BEAMFORMING

*Richard Stanton and Mike Brookes*

Imperial College London

{rs408, mike.brookes}@imperial.ac.uk

## ABSTRACT

Conventional beamformer design assumes that the phase differences between the received sensor signals are a deterministic function of the array and source geometry. In fact however, these phase differences are subject to random variations arising both from source and sensor position uncertainties and from fluctuations in sound velocity. We present a framework for modelling these uncertainties and show that improved beamformers are obtained when they are taken into account.

*Index Terms*— robust beamforming, distributed array, SNR beamformer, steering vector mismatch

## 1. INTRODUCTION

Conventional signal independent beamforming relies on the assumption that phase differences between the received sensor signals are a deterministic function of the source and sensor geometry. However, in practice, there are random deviations in the propagation paths and element positions that we cannot control and these result in additional correlated phase shifts in each channel. If we ignore these deviations, these phase shifts will degrade the performance of the beamformer [1]. By modelling these deviations, we can construct beamformers that are robust to these random phase changes.

Element position errors occur when the sensors or source locations are not precisely known. The errors cause a change in propagation distance and phase differences, in a similar way to steering vector mismatches. By identifying which element locations are less well defined than others we are able to utilise the most reliable sensors to avoid large phase uncertainties.

There are two main approaches to addressing this problem. In circumstances where the wanted signal can be clearly distinguished from the noise, it is possible to use adaptive signal-dependent methods to adjust the beamformer coefficients. When this is not the case however, it is necessary to use a signal-independent method that is robust to modelling uncertainties.

There have been several approaches in the literature to address this problem. Beamformers with improved robustness to array placement errors and steering errors have been

designed by considering microphone phase errors [2–4]. Derivative constraints have been used to prevent small deviations in the steering vector causing large degradation in performance [2, 5–8]. Diagonal loading of the array covariance matrix has been used to increase robustness to correlated errors [9–12]; this is similar to applying a constraint on the white noise gain [10]. Other signal dependent methods have involved iteratively converging to maximise the steering vector power [13–16]. Most robust beamformers consider uncorrelated error terms which appear on the diagonal of the array autocorrelation matrix. However beamformers that are robust to steering vector mismatches are not necessarily robust to any other type mismatch [17].

Channel uncertainty errors cause correlated errors terms. Modelling channel uncertainties is especially important when using distributed beamformers with widely separated sensors. It is a common assumption that the channel propagation speed between a source and two different sensors is identical. However when the arrays are far apart this no longer applies [18]. Because the channels may be widely separated in space, the variations can become large enough to cause phase differences that degrade the performance of the beamformer.

These considerations apply to any situation where there is uncertainty in wave propagation speed. For example, in the field of medical imaging, ultrasound scans can be adversely affected by speed-of-sound errors [19] and in sonar systems the propagation speed may vary greatly [20, 21].

Uncertainties in sensor positions or channel propagation speeds result in phase uncertainties whose magnitude is proportional to frequency. Thus the higher the frequency the larger the deviations and the less reliable is the corresponding sensor. In this paper we model these correlated and uncorrelated variations. Using these uncertainties we can design a more robust beamformer that utilises the most reliable sensors at each frequency.

## 2. BEAMFORMER WEIGHTS DESIGN

In each frequency band,  $k$ , we derive the beamformer output,  $y$ , as the weighted sum of the array data,  $\mathbf{x}$ :

$$y(k) = \mathbf{w}(k)^H \mathbf{x}(k),$$

where  $\mathbf{w}(k)$  is a vector of complex-valued weights. Since each frequency band is processed independently, the frequency index,  $k$ , has been omitted in most places in the remainder of this paper for clarity. We model the array data as follows:

$$\mathbf{x} = \mathbf{D}\mathbf{s} + \mathbf{v}, \quad (1)$$

$$\mathbf{v} = \mathbf{v}_s + \mathbf{v}_d, \quad (2)$$

where  $\mathbf{D} \in \mathbb{C}^{M \times P}$  are complex propagation coefficients from  $P$  sources to  $M$  sensors,  $\mathbf{s} \in \mathbb{C}^{P \times 1}$  is the source data,  $\mathbf{v}_s \in \mathbb{C}^{M \times 1}$  is white Gaussian sensor noise and  $\mathbf{v}_d \in \mathbb{C}^{M \times 1}$  is spatially diffuse acoustic noise. The first source,  $s_1$ , is considered the desired source and the remaining sources,  $s_2, \dots, s_P$ , are considered interferers.

Classical data-dependent beamformer weights are derived as a function of the array data correlation,  $\langle \mathbf{x}\mathbf{x}^H \rangle$ , where  $\langle \cdot \cdot \rangle$  denotes the expected value. In this paper, we extend the array data model to introduce an unknown random phase contribution to each of the propagation coefficients:

$$\mathbf{D} = \bar{\mathbf{D}} \odot \exp(j\omega_k \mathbf{T}), \quad (3)$$

where  $\odot$  denotes element-by-element multiplication,  $\omega_k$  represents the angular frequency relating to frequency index  $k$ ,  $\mathbf{T}$  represents the zero-mean Gaussian variations in the propagation path time delays and  $\bar{\mathbf{D}}$  represents the propagation coefficients from the conventional deterministic model. Using (1) and (3) we can expand  $\langle \mathbf{x}\mathbf{x}^H \rangle$  as

$$\begin{aligned} \langle \mathbf{x}\mathbf{x}^H \rangle &= \langle \mathbf{D}\mathbf{S}\mathbf{D}^H \rangle + \langle \mathbf{v}\mathbf{v}^H \rangle \\ &= \left\langle (\bar{\mathbf{D}} \odot \exp(j\omega_k \mathbf{T})) \mathbf{S} (\bar{\mathbf{D}} \odot \exp(j\omega_k \mathbf{T}))^H \right\rangle \\ &\quad + \langle \mathbf{v}\mathbf{v}^H \rangle, \end{aligned} \quad (4)$$

where  $\mathbf{S} = \langle \mathbf{s}\mathbf{s}^H \rangle$ . Assuming that all sources are independent we have:

$$\mathbf{S} = \text{diag}(\langle s_1^2 \rangle \dots \langle s_P^2 \rangle).$$

We can expand the first term in (4) as

$$\left\langle (\bar{\mathbf{D}} \odot \exp(j\omega_k \mathbf{T})) \mathbf{S} (\bar{\mathbf{D}} \odot \exp(j\omega_k \mathbf{T}))^H \right\rangle = \mathbf{A},$$

where the elements of  $\mathbf{A}$  are now given by

$$\begin{aligned} a_{i,j} &= \sum_{p=1}^P \bar{d}_{ip} \bar{d}_{jp}^* \langle s_p^2 \rangle \langle \exp(j\omega_k (t_{ip} - t_{jp})) \rangle \\ &= \sum_{p=1}^P \bar{d}_{ip} \bar{d}_{jp}^* \langle s_p^2 \rangle \exp\left(-\frac{\omega_k^2}{2} \langle (t_{ip} - t_{jp})^2 \rangle\right) \\ &= \sum_{p=1}^P \bar{d}_{ip} \bar{d}_{jp}^* \langle s_p^2 \rangle \\ &\quad \times \exp\left(-\frac{\omega_k^2}{2} (\langle t_{ip}^2 \rangle + \langle t_{jp}^2 \rangle - 2 \langle t_{ip} t_{jp} \rangle)\right), \end{aligned} \quad (5)$$

in which  $\bar{d}_{ip}$  and  $t_{ip}$  are elements of  $\bar{\mathbf{D}}$  and  $\mathbf{T}$  respectively. From the above we see that we need to determine the correlations,  $\langle t_{ip} t_{jp} \rangle$ , between the elements of  $\mathbf{T}$  that represent the propagation time uncertainties from source  $p$  to sensors  $i$  and  $j$  respectively.

### 3. PATH UNCERTAINTIES

Variations in the propagation time from source  $p$  to sensors  $i$  and  $j$ ,  $t_{ip}$  and  $t_{jp}$ , can arise from uncertainties in either source/sensor locations or in channel propagation speed. We assume these two effects to be independent so that the covariance  $\langle t_{ip} t_{jp} \rangle$  may be expressed as a sum:

$$\langle t_{ip} t_{jp} \rangle = \langle t_{ip} t_{jp} \rangle_S + \langle t_{ip} t_{jp} \rangle_C. \quad (6)$$

We discuss these two terms separately below.

#### 3.1. Position deviations

If we have a source at  $\mathbf{p}_p + \bar{\mathbf{p}}_p$  and a sensor at  $\mathbf{m}_i + \bar{\mathbf{m}}_i$  where  $\bar{\mathbf{p}}_p$  and  $\bar{\mathbf{m}}_i$  are zero-mean deviations from the nominal positions, then the change in path length due to  $\bar{\mathbf{p}}_p$  and  $\bar{\mathbf{m}}_i$  is the component of  $(\bar{\mathbf{m}}_i - \bar{\mathbf{p}}_p)$  in the direction of  $(\mathbf{m}_i - \mathbf{p}_p)$ :

$$\delta(i, p) = \frac{(\mathbf{m}_i - \mathbf{p}_p)^T (\bar{\mathbf{m}}_i - \bar{\mathbf{p}}_p)}{|\mathbf{m}_i - \mathbf{p}_p|}.$$

The path length correlation is therefore:

$$\begin{aligned} \langle \delta(i, p) \delta(j, p) \rangle &= \frac{1}{|\mathbf{m}_i - \mathbf{p}_p| |\mathbf{m}_j - \mathbf{p}_p|} \dots \\ &(\mathbf{m}_i - \mathbf{p}_p)^T (\langle \bar{\mathbf{m}}_i \bar{\mathbf{m}}_j^T \rangle + \langle \bar{\mathbf{p}}_p \bar{\mathbf{p}}_p^T \rangle) (\mathbf{m}_j - \mathbf{p}_p), \end{aligned}$$

where we assume in the final line that the source and sensor deviations are independent. If, in addition, the position deviations are isotropic, we can write  $\langle \bar{\mathbf{m}} \bar{\mathbf{m}}^T \rangle = \sigma_m^2 \mathbf{I}$  and  $\langle \bar{\mathbf{p}} \bar{\mathbf{p}}^T \rangle = \sigma_p^2 \mathbf{I}$  which results in  $\langle \delta(i, p) \delta(j, p) \rangle = \sigma_m^2 + \sigma_p^2$ .

For solving the general case, we note that the change in path length causes a change in the propagation path time as in (5) which is given by:

$$\langle t_{ip} t_{jp} \rangle_S = \frac{1}{c^2} \langle \delta(i, p) \delta(j, p) \rangle. \quad (7)$$

#### 3.2. Channel deviation

The deviation in sound propagation speed is a function of position and can be modelled as follows:

$$\frac{1}{c(\mathbf{x})} = \frac{1}{c_0} + g(\mathbf{x}),$$

where the quantity  $\frac{1}{c_0}$  is the mean inverse velocity (note that  $c_0$  will not in general equal the mean velocity) and the deviation from this value,  $g(\mathbf{x})$ , is zero mean.

The total path delay from  $\mathbf{x} = \mathbf{a}$  to  $\mathbf{x} = \mathbf{b}$  is given by:

$$q(\mathbf{a}, \mathbf{b}) = \frac{|\mathbf{b} - \mathbf{a}|}{c_0} + |\mathbf{b} - \mathbf{a}| \int_{t=0}^1 g(\mathbf{a} + (\mathbf{b} - \mathbf{a})t) dt. \quad (8)$$

We assume that  $g(\mathbf{x})$  is zero-mean, spatially stationary and isotropic and that it follows a 3-dimensional spatial Gaussian distribution with covariance

$$\langle g(\mathbf{x})g(\mathbf{y}) \rangle = \kappa^2 \exp\left(-\frac{|\mathbf{x} - \mathbf{y}|^2}{2\sigma^2}\right)$$

that is characterised by the two parameters  $\kappa^2 = \langle g(\mathbf{x})g(\mathbf{x}) \rangle$  and  $\sigma^2$  which define its variance and spatial extent respectively.

If we consider two paths starting from the same point (which, without loss of generality, we can take to be the origin), it is possible to express their covariance as a single line integral:

$$\begin{aligned} & \left\langle \left( (q(0, \mathbf{a}) - \frac{|\mathbf{a}|}{c_0}) \left( (q(0, \mathbf{b}) - \frac{|\mathbf{b}|}{c_0})^* \right) \right) \right\rangle \quad (9) \\ &= |\mathbf{a}| |\mathbf{b}| \int_{s=0}^1 \int_{t=0}^1 \langle g(\mathbf{a}s) g(\mathbf{b}t) \rangle dt ds \\ &= 2\pi\kappa^2\sigma^2 \dots \\ & \int_{s=0}^1 \mathcal{N} \left( s \sqrt{1 - \left( \frac{\mathbf{b}^T \mathbf{a}}{|\mathbf{a}| |\mathbf{b}|} \right)^2}; 0, \frac{\sigma^2}{|\mathbf{a}|^2} \right) \dots \\ & \left( \Phi \left( \frac{|\mathbf{b}|^2 - \mathbf{b}^T \mathbf{a}s}{\sigma |\mathbf{b}|} \right) - \Phi \left( \frac{-\mathbf{b}^T \mathbf{a}s}{\sigma |\mathbf{b}|} \right) \right) ds, \end{aligned}$$

where  $\mathcal{N}(x; \mu, \sigma^2)$  represents a Gaussian Probability Density Function (PDF) and  $\Phi(x)$  is the cumulative Gaussian distribution. The detailed derivation of (9) is straightforward but too length to include in this paper.

The covariance between the elements of  $\mathbf{T}$  representing the delays from source  $p$  to sensors  $i$  and  $j$  is therefore

$$\begin{aligned} \langle t_{ip}t_{jp} \rangle_C &= \left\langle \left( (q(0, \mathbf{m}_i - \mathbf{p}_p) - \frac{|\mathbf{m}_i - \mathbf{p}_p|}{c_0}) \right) \right. \quad (10) \\ & \left. \left( (q(0, \mathbf{m}_j - \mathbf{p}_p) - \frac{|\mathbf{m}_j - \mathbf{p}_p|}{c_0})^* \right) \right\rangle, \end{aligned}$$

where  $\mathbf{m}_i$  is the position vector of sensor  $i$  and  $\mathbf{p}_p$  source  $p$ .

## 4. SIMULATIONS

Applying (6) to a distributed beamformer shows how the weights are changed when we consider the random deviations.

### 4.1. Four Element Array

We consider the distributed beamformer consisting of four sensors, as illustrated in Fig. 1. A single source is at position (0.5 m 0.5 m). Sensor  $M1$  is placed at a distance of

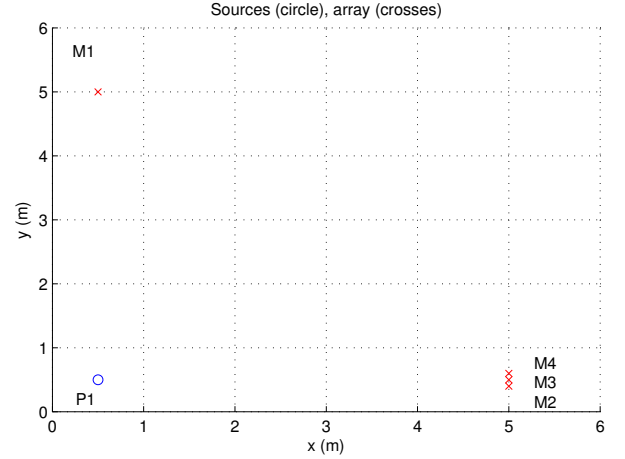


Fig. 1. Sensor and source locations within a room

5 m above the source. Sensors  $M2$ ,  $M3$  and  $M4$ , are placed, perpendicular to  $M1$ , approximately along the same path, at distances of 0.4 m, 0.5 m and 0.6 m from the  $y$ -axis respectively. Based on experimental data we have used  $\sigma = 0.2$  and  $\kappa^2 = 1.7 \times 10^{-8}$  in the simulations. The corresponding correlations from (9) are given by

$$\langle t_{ip}t_{jp} \rangle_C = 5.15 \times 10^{-8} \begin{bmatrix} 1 & 0.041 & 0.041 & 0.043 \\ 0.041 & 1 & 0.981 & 0.924 \\ 0.041 & 0.981 & 1 & 0.981 \\ 0.043 & 0.924 & 0.981 & 1 \end{bmatrix}. \quad (11)$$

The paths from the source to sensors  $M2$ ,  $M3$  and  $M4$  approximately coincide and we see from the above correlation matrix that their delays are strongly correlated. In contrast, the path from the source to  $M1$  does not overlap the paths to the other sensors and we see from the low off-diagonal values in the first row and column that the delays are largely uncorrelated. Fig. 2 shows the correlation of  $x_3$  and  $x_j$  in the absence of noise,  $a_{3,j}$ , as a function of frequency, according to (5). The bottom line represents sensor  $M1$ , its correlation decreases with frequency faster than that of  $M2$  and  $M4$ , which are represented by the middle lines.

### 4.2. General Case

Utilising the change in correlation we can design beamformer weights that are robust to these channel deviations in a given array geometry.

To illustrate these effects, we compare two alternative designs of the maximal Signal-to-Noise Ratio (SNR) beamformer [22, 23]. The optimal weights are the entries of the eigenvector corresponding to the maximal eigenvalue,  $\lambda_{max}$ , of the matrix  $\mathbf{B}$ :

$$\begin{aligned} \mathbf{B} &= \langle \mathbf{v}\mathbf{v}^H \rangle^{-1} \langle \mathbf{D}\mathbf{S}\mathbf{D}^H \rangle \\ \mathbf{B}\mathbf{w} &= \lambda_{max}\mathbf{w}, \end{aligned} \quad (12)$$

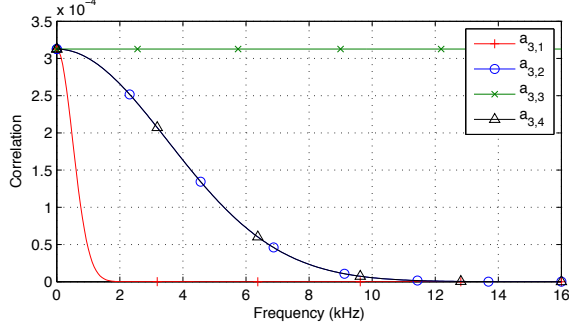


**Fig. 2.** Correlation between sensor signals  $x_3$  and  $x_j$  in the absence of noise,  $a_{3,j}$ .

First, the original weights, when the propagation coefficients are taken from the conventional deterministic model,

$$\mathbf{D} = \bar{\mathbf{D}}, \quad (13)$$

and second, the proposed weights, when we include the random deviations matrix from (3):

$$\mathbf{D} = \bar{\mathbf{D}} \odot \exp(j\omega_k \mathbf{T}). \quad (14)$$

The source power is assumed constant over frequency corresponding to 0 dB at a distance of 1 m. We test each beamformers in the presence of  $-10$  dB of Gaussian sensor noise and  $-10$  dB of diffuse noise at the sensor. The diffuse noise correlation used in the simulations is given as follows [24,25]:

$$\langle \mathbf{v}_d \mathbf{v}_d^* \rangle_{(i,j)} = \phi_d \frac{\sin\left(\frac{\omega_k}{c} |\mathbf{m}_i - \mathbf{m}_j|\right)}{\frac{\omega_k}{c} |\mathbf{m}_i - \mathbf{m}_j|},$$

where  $|\mathbf{m}_i - \mathbf{m}_j|$  is the absolute distance between sensors  $i$  and  $j$  and  $\phi_d$  is the expected power of the diffuse field.

To compare the two approaches we compute the SNR of each beamformer:

$$\text{SNR}(k) = \frac{\mathbf{w}^H \langle \mathbf{D} \langle \mathbf{s} \mathbf{s}^H \rangle \mathbf{D}^H \rangle \mathbf{w}}{\mathbf{w}^H \langle \langle \mathbf{v} \mathbf{v}^H \rangle \rangle \mathbf{w}},$$

where  $\mathbf{D} = \bar{\mathbf{D}} \odot \exp(j\omega_k \mathbf{T})$ . Fig. 3 shows the improvement in SNR comparing (13) and (14) across 300 random array geometries, with one source, for different numbers of sensors. The mean gain of the robust beamformer weights against the conventional weights increases with frequency. The more sensors present, the more beneficial the robust weights. As frequency increases, the expected channel deviation errors grow. Thus the performance of the conventional method, (13), starts to degrade. However the robust weights design, (14), still performs well, thus the SNR increases with frequency. Also the robust beamformer never degrades performance.

Fig. 4 shows that if we include errors in all source and sensor positions, using  $\sigma_m = 0.05$  and  $\sigma_p = 0.05$ , we see further gains in the performance over the conventional beamformer,

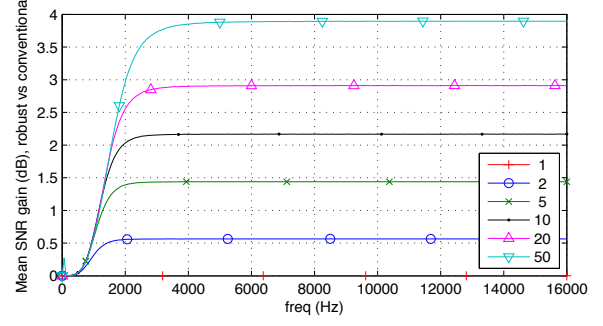


**Fig. 3.** The mean SNR gain of the robust beamformer, including channel deviations, compared to the conventional beamformer against frequency, for different numbers of sensors.

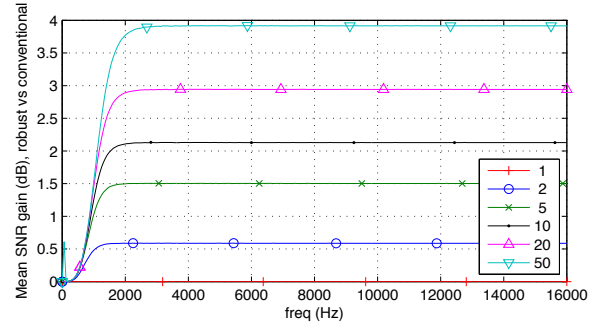


**Fig. 4.** The mean SNR gain of the robust beamformer, including channel deviations and position errors, compared to the conventional beamformer against frequency, for different numbers of sensors.

particularly at lower frequencies ( $< 2$  kHz). The position errors cause an additional phase difference that increases with frequency. The performance of the proposed robust weights are not affected as much. Thus the SNR gains are further improved with frequency.

## 5. CONCLUSIONS

In this paper we have presented a model for the propagation delay variability that affects the signals received by an acoustic array as a result of fluctuations in sound speed and uncertainties in the locations of sources and sensors. We have shown how this model can be used to derive an explicit formula for the correlation matrix of the propagation delays from an arbitrary source position to the elements of a sensor array. By incorporating this into the conventional SNR beamformer design procedure, we have demonstrated that it always results in performance improvements especially at high frequencies where the resultant phase uncertainties are greatest.

## REFERENCES

- [1] R. Compton, Jr., "The effect of random steering vector errors in the applebaum adaptive array," *IEEE Trans. Aerosp. Electron. Syst.*, no. 4, pp. 392–400, 1982.
- [2] G.T. Zunic and L.J. Griffiths, "A robust method in adaptive array processing for random phase errors," in *Proc. IEEE Intl. Conf. on Acoustics, Speech and Signal Processing (ICASSP)*. IEEE, 1991, pp. 1357–1360.
- [3] S. Doclo and M. Moonen, "Design of broadband beamformers robust against gain and phase errors in the microphone array characteristics," *IEEE Trans. Signal Process.*, vol. 51, no. 10, pp. 2511–2526, 2003.
- [4] C.C. Lai, S. Nordholm, and Y.H. Leung, "Design of robust steerable broadband beamformers incorporating microphone gain and phase error characteristics," in *Proc. IEEE Intl. Conf. on Acoustics, Speech and Signal Processing (ICASSP)*. IEEE, 2011, pp. 101–104.
- [5] M. Er and A. Cantoni, "Derivative constraints for broad-band element space antenna array processors," *IEEE Trans. Acoust., Speech, Signal Process.*, vol. 31, no. 6, pp. 1378–1393, Dec. 1983.
- [6] K.C. Huarng and C.C. Yeh, "Performance analysis of derivative constraint adaptive arrays with pointing errors," *IEEE Trans. Acoust., Speech, Signal Process.*, vol. 38, no. 2, pp. 209–219, Feb. 1990.
- [7] O.L. Frost, III, "An algorithm for linearly constrained adaptive array processing," *Proc. IEEE*, vol. 60, no. 8, pp. 926–935, Aug. 1972.
- [8] K.M. Buckley and L.J. Griffiths, "An adaptive generalized sidelobe canceller with derivative constraints," *IEEE Trans. Antennas Propag.*, vol. 34, no. 3, pp. 311–319, 1986.
- [9] J. Li, P. Stoica, and Z. Wang, "On robust capon beamforming and diagonal loading," *IEEE Trans. Signal Process.*, vol. 51, no. 7, pp. 1702–1715, 2003.
- [10] H. Cox, R.M. Zeskind, and M.M. Owen, "Robust adaptive beamforming," *IEEE Trans. Acoust., Speech, Signal Process.*, vol. 35, no. 10, pp. 1365–1376, Oct. 1987.
- [11] B.D. Carlson, "Covariance matrix estimation errors and diagonal loading in adaptive arrays," *IEEE Trans. Aerosp. Electron. Syst.*, vol. 24, no. 4, pp. 397–401, 1988.
- [12] A.B. Gershman, Z.Q. Luo, S. Shahbazpanahi, and S.A. Vorobyov, "Robust adaptive beamforming using worst-case performance optimization," in *Proc. Asilomar Conference on Signals, Systems and Computers, 2003*. IEEE, 2003, vol. 2, pp. 1353–1357.
- [13] S.E. Nai, W. Ser, Z.L. Yu, and H. Chen, "Iterative robust minimum variance beamforming," *IEEE Trans. Signal Process.*, vol. 59, no. 4, pp. 1601–1611, 2011.
- [14] S.A. Vorobyov, A.B. Gershman, and Z.Q. Luo, "Robust adaptive beamforming using worst-case performance optimization: A solution to the signal mismatch problem," *IEEE Trans. Signal Process.*, vol. 51, no. 2, pp. 313–324, 2003.
- [15] R.G. Lorenz and S.P. Boyd, "Robust minimum variance beamforming," *IEEE Trans. Signal Process.*, vol. 53, no. 5, pp. 1684–1696, 2005.
- [16] M.H. Er and B.C. Ng, "A new approach to robust beamforming in the presence of steering vector errors," *IEEE Trans. Signal Process.*, vol. 42, no. 7, pp. 1826–1829, 1994.
- [17] A.B. Gershman, "Robust adaptive beamforming in sensor arrays," *AEU International Journal of Electronics and Communications*, vol. 53, no. 6, pp. 305–314, 1999.
- [18] P. Annibale, J. Filos, P.A. Naylor, and R. Rabebstein, "TDOA-based speed of sound estimation for air temperature and room geometry inference," *IEEE Trans. Audio, Speech, Lang. Process.*, vol. 21, no. 2, pp. 234–246, feb 2013.
- [19] M.E. Anderson, M.S. McKeag, and G.E. Trahey, "The impact of sound speed errors on medical ultrasound imaging," *The Journal of the Acoustical Society of America*, vol. 107, pp. 3540, 2000.
- [20] V.A. Del Grosso and C.W. Mader, "Speed of sound in pure water," *the Journal of the Acoustical Society of America*, vol. 52, pp. 1442, 1972.
- [21] W. Wagner and A. Pruß, "The IAPWS formulation 1995 for the thermodynamic properties of ordinary water substance for general and scientific use," *Journal of Physical and Chemical Reference Data*, vol. 31, pp. 387, 2002.
- [22] B.D. van Veen and K.M. Buckley, "Beamforming: A versatile approach to spatial filtering," *IEEE Acoustics, Speech and Signal Magazine*, vol. 5, no. 2, pp. 4–24, Apr. 1988.
- [23] D. Monzingo and T.W. Miller, *Introduction to Adaptive Arrays*, Wiley, New York, USA, 1980.
- [24] B.F. Cron and C.H. Sherman, "Spatial-correlation functions for various noise models," *J. Acoust. Soc. Am.*, vol. 34, no. 11, pp. 1732–1736, Nov. 1962.
- [25] R.K. Cook, R.V. Waterhouse, R.D. Berendt, S. Edelman, and M.C. Thompson, "Measurement of correlation coefficients in reverberant sound fields," *J. Acoust. Soc. Am.*, vol. 27, no. 6, pp. 1072–1077, 1955.